Bled Workshops
in Physics
Vol. 15, No. 1
p. 28

Proceedings of the Mini-Workshop
Quark Masses and Hadron Spectra
Bled, Slovenia, July 6 - 13, 2014

Overlap quark propagator in Coulomb-gauge QCD*

Y. Delgado[a], M. Pak[a], M. Schröck[b]

[a] Institut für Physik, Karl-Franzenz Universität Graz, 8010 Graz, Austria
[b] Istituto Nazionale di Fisica Nucleare (INFN), Sezione di Roma Tre, Rome, Italy

Abstract. The quark propagator is examined on quenched gauge field configurations in Coulomb Gauge using chirally symmetric Overlap fermions. In this gauge the dressing functions of the quark propagator can be related to the confinement and chiral symmetry properties of QCD. Confinement can be attributed to the infrared divergent vector dressing function. The dressing functions of the quark propagator are evaluated, the dynamical quark mass is extracted and the chiral extrapolation of these quantities is performed. Furthermore, the issue of Dirac low-mode removal is discussed.

1 Introduction

The quark propagator is the central object for computing hadronic correlators, from which baryon and meson masses are extracted. In the continuum approach, it is the central ingredient for the Bethe–Salper equation. The gauge has to be fixed in order to analyze its behavior. We choose Coulomb gauge, where the longitudinal part of the gauge field is eliminated and the so-called color-Coulomb potential arises, which is the QCD analogue of the QED Coulomb potential and which describes the interaction between two static color sources. Continuum methods in Coulomb gauge, especially the variational approach, Ref. [1], have been used mainly to study the pure Yang-Mills part of the theory.

Although progress has been made also in the quark sector in recent years, Refs. [2, 3], the quark propagator in Coulomb gauge is not yet well understood. Lattice studies are highly needed, especially to improve on the still widely used rainbow-ladder Dyson-Schwinger equations. The only lattice study in this direction has been performed in Ref. [4]. We use Overlap fermions for this purpose, which allow for a clear and unambiguous examination of the dressing functions. With non-chiral fermions tree-level corrections and improvement techniques have to be applied. Overlap Dirac propagator studies in Landau gauge can be found in Refs. [5, 6].

Another motivation of this work is to explore a phase, where chiral symmetry is restored by hand in the vacuum. What happens to the confinement properties in such a situation? We argue that we get a clearer picture of this issue by analyzing the dressing functions of the quark propagator.

* Talk delivered by M. Pak

This contribution is organized as follows: In Chapter 2 the Overlap Dirac operator is introduced and in chapter 3 the lattice setup is discussed. In Chapter 4 the main features of the Coulomb gauge quark propagator and our lattice results are presented. The issue of low-mode removal is shortly discussed. In Chapter 5 a conclusion and an outlook are given.

2 Overlap Dirac operator and free propagator

We use the following parameterization for the massive Overlap Dirac operator, Ref. [7],

$$D(m_0) = \left(1 - \frac{m_0}{2\rho}\right) D(0) + m_0 \,, \tag{1}$$

with

$$D(0) = \rho \left(\mathbb{1} + \gamma_5 \,\mathrm{sign}\left[H_W(-\rho)\right]\right) \,, \tag{2}$$

where $H_W(-\rho) = a\gamma_5 D_W(-\rho)$ is the Hermitian Wilson-Dirac operator, m_0 the mass parameter and ρ the negative mass of the Wilson-Dirac operator, which is set to the value 1.6 throughout this work. The massless Ovelap-Dirac operator $D(0)$ is an explicit solution of the Ginsparg-Wilson equation and therefore describes exactly massless quarks on the lattice. The eigenvalues lie on a circle in the complex plane with radius ρ. Exact zero modes occur and a lattice version of the index theorem can be defined, see Ref. [8].

To make contact with continuum physics, we impose for the massless Overlap propagator

$$\widetilde{S} = S - \frac{1}{2\rho} \,, \tag{3}$$

from which continuum chiral symmetry follows. The structure of the free (massive) propagator is given as

$$\left(\widetilde{S}^{(0)}\right)^{-1}(p) = i\gamma_\mu q_\mu + \mathbb{1} m \,. \tag{4}$$

The Overlap lattice momentum q_μ and current quark mass m are computed as

$$q_\mu = \frac{4\rho^2}{(2\rho - m_0)} \frac{k_\mu \left(\sqrt{k_\mu^2 + A^2} + A\right)}{k_\mu^2} \,, \quad m = \frac{m_0}{1 - \frac{m_0}{2\rho}} \,, \tag{5}$$

which can be obtained from Eq. (4) and which are used in the extraction of the lattice dressing functions.

3 Lattice setup

Using the Chroma software package [9] and QDP-JIT [10, 11], configurations are generated on a 20^4 lattice at $\beta = 7.552$ ($a = 0.2$ fm) with the Lüscher-Weisz [12]

gauge action. The configurations are then fixed to Coulomb gauge ($\partial_i A_i = 0$). However, the temporal links are not affected by this procedure and are fixed to the Integrated Polyakov loop gauge. For further details, see Ref. [13].

With an ensemble of 96 configurations we evaluate the quark propagator for six current quark masses chosen at $m = (0.085, 0.092, 0.099, 0.113, 0.137, 0.173)$ GeV. The Dirac matrix is inverted on point sources for each configuration. Subsequently, the quark propagators are transformed to momentum space after which the extraction of the dressing functions is performed according to the description given in [4, 14].

4 Non-perturbative quark propagator

In Coulomb gauge the non-perturbative quark propagator is parameterized by four independent dressing functions

$$S^{-1}(\mathbf{p}, p_4) = i\gamma_i p_i A_S(\mathbf{p}) + i\gamma_4 p_4 A_T(\mathbf{p}) + \gamma_4 p_4 \gamma_i p_i A_D(\mathbf{p}) + \mathbb{1} B(\mathbf{p}) \,. \qquad (6)$$

Here A_S, A_T, A_D, B are *spatial*, *temporal*, *mixed* and *scalar* dressing functions, respectively. We observe that *all* dressing functions are independent of p_4, which was also observed in Ref. [4]. We note that the temporal part $A_T(\mathbf{p})$ vanishes if the additional gauge freedom with respect to space independent gauge transformations is not fixed. A possible mixed component $A_D(\mathbf{p})$, which does not appear at tree-level, also seems to vanish non-perturbatively, see left-hand side of Fig. 1. The temporal dressing function $A_T(\mathbf{p})$, which does not depend on the Coulomb gauge condition, seems to approach a finite value in the IR, although the error bars are too large to make a precise statement, see right-hand side of Fig. 1.

From mean-field studies in continuum Coulomb gauge it is argued that, due to the presence of the linear confinement potential, the scalar and vector dressing functions diverge as $|\mathbf{p}| \to 0$, see Ref. [15]. However, the dynamical quark mass $M(\mathbf{p}) = B(\mathbf{p})/A_S(\mathbf{p})$ becomes constant for $|\mathbf{p}| \to 0$, identified as the constituent quark mass. This is a remarkable result: the divergencies in the dressing functions have to cancel each other to give a finite infrared mass. Since the lattice imposes an infrared regulator, we do not observe a divergence. However, we observe that both dressing functions $B(\mathbf{p})$ and $A_S(\mathbf{p})$ increase for small momenta, see Fig. 2. It can be seen, that in the chiral limit a non-vanishing scalar dressing function appears. This is a clear signal for chiral symmetry breaking and dynamical mass generation. From the dynamical mass function $M(\mathbf{p})$ in Fig. 3, we observe that around 1 GeV mass generation sets in and that a constituent mass for chiral quarks around 300 MeV is reached.

Finally let us comment on an interesting observation in Coulomb gauge. Since all dressing functions are independent of p_4, the static quark propagator can be evaluated, yielding

$$S(\mathbf{p}) = \frac{B(\mathbf{p}) - i\boldsymbol{\gamma} \cdot \mathbf{p} A_S(\mathbf{p})}{2\omega(\mathbf{p})}, \qquad (7)$$

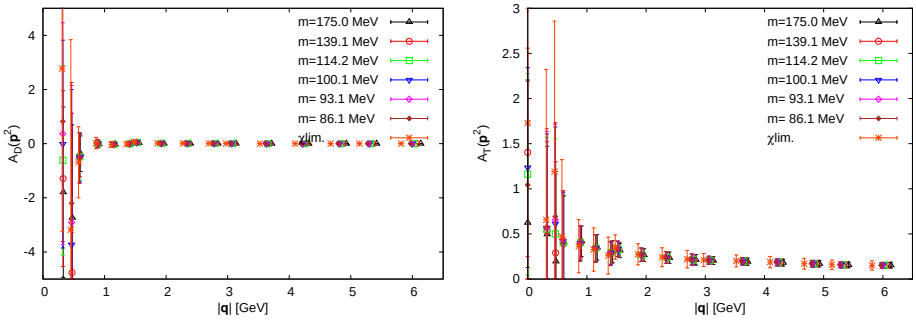

Fig. 1. *Mixed component* $A_D(\mathbf{p})$ *(l.h.s.) and temporal component* $A_T(\mathbf{p})$ *(r.h.s.) for several current quark masses* m *and in the chiral limit.*

and the quark dispersion relation $\omega(\mathbf{p})$ is identified as

$$\omega(\mathbf{p}) = A_T(\mathbf{p})A_S(\mathbf{p})\sqrt{\mathbf{p}^2 + M^2(\mathbf{p})}\,. \tag{8}$$

Since the vector dressing functions $A_S(\mathbf{p})$ is a divergent quantity in the infrared, the energy dispersion $\omega(\mathbf{p})$ is divergent as well. This issue has a clear physical implication: the excitation energy of a confined quark is infinite. Such a mechanism of quark confinement makes Coulomb gauge appealing.

Now a question arises: if one removes the chiral condensate from the quark propagator, is the energy dispersion $\omega(\mathbf{p})$ still infrared divergent? If yes, then confinement is intact, although chiral symmetry has been artificially restored in the vacuum. We expect that, after chiral symmetry restoration, the quark condensate $\langle\overline{\psi}\psi\rangle$ and therefore the dynamical quark mass $M(\mathbf{p})$ as well as the scalar dressing function $B(\mathbf{p})$ vanish in the chiral limit. However, the interesting question will be, how the vector dressing function $A_S(\mathbf{p})$ is affected by artificial chiral symmetry restoration. First results show that the spatial dressing function does not change its shape. This suggests that $A_S(\mathbf{p})$ is still infrared divergent in the continuum limit. A single quark is still removed from the spectrum. This conclusion supports recent hadron spectroscopy studies, see Refs. [16, 17]. Our final results on this issue will be presented elsewhere, Ref. [18].

5 Summary and conclusions

First steps in a detailed analysis of the Overlap quark propagator in Coulomb gauge have been presented. A clear indication of dynamical mass generation is observed and a constituent mass around 300 MeV is obtained. Scalar and vector dressing functions increase for small momenta. If a divergent behavior is present has to be left to a future work. Moreover, it is shown that in Coulomb gauge confinement and chiral symmetry breaking can be linked to each other by a quark dispersion relation. It is shown that via the vector dressing function it can be judged if confinement is still intact when chiral symmetry is artificially restored by removing the low-lying Dirac eigenmodes from the spectrum.

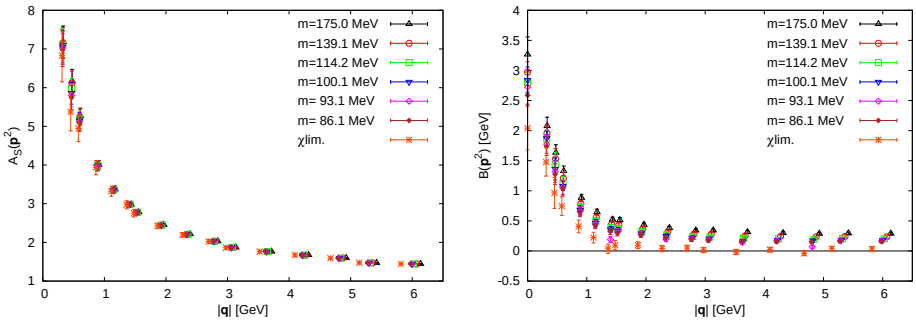

Fig. 2. *Spatial component* $A_S(\mathbf{p})$ *(l.h.s.) and scalar component* $B(\mathbf{p})$ *(r.h.s) for several quark masses* m *and in the chiral limit.*

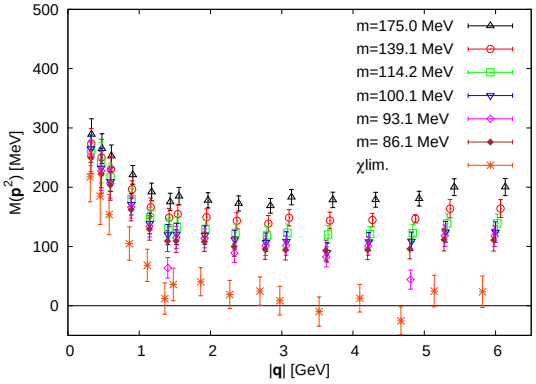

Fig. 3. *Dynamical mass function* $M(\mathbf{p})$ *for several quark masses* m *and in the chiral limit.*

Acknowledgments. Discussions with G. Burgio and L. Glozman are greatly acknowledged. M.P. acknowledges support by the Austrian Science Fund (FWF) through the grant P26627-N27. The calculations have been performed on clusters at ZID at the University of Graz and at the Graz University of Technology.

References

1. C. Feuchter and H. Reinhardt, Phys. Rev. D **70**, 105021 (2004) [hep-th/0408236].
2. M. Pak and H. Reinhardt, Phys. Lett. B **707**, 566 (2012) [arXiv:1107.5263 [hep-ph]].
3. M. Pak and H. Reinhardt, Phys. Rev. D **88**, 125021 (2013) [arXiv:1310.1797 [hep-ph]].
4. G. Burgio, M. Schröck, H. Reinhardt and M. Quandt, Phys. Rev. D **86**, 014506 (2012) [arXiv:1204.0716 [hep-lat]].
5. F. D. R. Bonnet *et al.* [CSSM Lattice Collaboration], Phys. Rev. D **65**, 114503 (2002) [hep-lat/0202003].
6. J. B. Zhang *et al.* [CSSM Lattice Collaboration], Phys. Rev. D **70**, 034505 (2004) [hep-lat/0301018].
7. H. Neuberger, Phys. Lett. B **417**, 141 (1998) [hep-lat/9707022].
8. P. Hasenfratz, V. Laliena and F. Niedermayer, Phys. Lett. B **427**, 125 (1998) [hep-lat/9801021].

9. R. G. Edwards *et al.* [SciDAC and LHPC and UKQCD Collaborations], Nucl. Phys. Proc. Suppl. **140**, 832 (2005) [hep-lat/0409003].
10. F. Winter, PoS LATTICE **2013**, 042 (2013).
11. F. T. Winter, M. A. Clark, R. G. Edwards and B. Joó, arXiv:1408.5925 [hep-lat].
12. M. Lüscher and P. Weisz, Commun. Math. Phys. **97**, 59 (1985) [Erratum-ibid. **98**, 433 (1985)].
13. G. Burgio, M. Quandt and H. Reinhardt, Phys. Rev. Lett. **102**, 032002 (2009) [arXiv:0807.3291 [hep-lat]].
14. J. I. Skullerud and A. G. Williams, Nucl. Phys. Proc. Suppl. **83**, 209 (2000) [hep-lat/9909142].
15. R. Alkofer and P. A. Amundsen, Nucl. Phys. B **306**, 305 (1988).
16. C. B. Lang and M. Schröck, Phys. Rev. D **84**, 087704 (2011) [arXiv:1107.5195 [hep-lat]].
17. L. Y. Glozman, C. B. Lang and M. Schröck, Phys. Rev. D **86**, 014507 (2012) [arXiv:1205.4887 [hep-lat]].
18. Y. Delgado Mercado, M. Pak and M. Schröck, in preparation.

Kvarkovski propagator v coulombski umeritvi kvantne kromodinamike

Y. Delgado[a], M. Pak[a], M. Schröck[b]

[a] Institut für Physik, Karl-Franzenz Universität Graz, 8010 Graz, Austria
[b] Istituto Nazionale di Fisica Nucleare (INFN), Sezione di Roma Tre, Rome, Italy

Proučujemo kvarkovski propagator na konfiguracijah gašenega umeritvenega polja v coulombski umeritvi. Pri tem uporabimo kiralno simetrične "prekrivalne fermione". V tej umeritvi lahko povežemo "funkcijo oblačenja" kvarkovskega propagatorja s priporom in kiralno simetrijo kromodinamike. Pripor lahko pripišemo infrardeče divergentni vektorski "funkciji oblačenja". Izvrednotimo "funkcije oblačenja" kvarkovskega propagatorja, razberemo dinamično maso kvarka in ekstrapoliramo vse te količine proti kiralni limiti. Končno razpravljamo, kako se odstranijo nizke Diracove ekscitacije.

Mase oblečenih kvarkov in barionska spektroskopija

W. Plessas

Theoretical Physics, Institute of Physics, University of Graz, A-8010 Graz, Austria

Prikažemo hierarhijo mas oblečenih kvarkov, ki prevladujejo v efektivnih modelih kvantne kromodinamike, zlasti v relativističnem modelu z oblečenimi kvarki. Opazimo, da je presežek dinamično generirane mase nad golo maso bolj ali manj neodvisen od okusa kvarkov in znaša $\Delta m \approx (370 \pm 30)$ MeV. Podobne vrednosti dajo tudi alternativni efektivni opisi barionske spektroskopije, na primer Dyson-Schwingerjev pristop.

Primerjava jedrskih potencialov za hiperon Lambda in za nukleon

Bogdan Povh[a] in Mitja Rosina[b,c]

[a] Max-Planck-Institut für Kernphysik, Postfach 103980, D-69029 Heidelberg, Germany
[b] Fakulteta za matematiko in fiziko, Univerza v Ljubljani, Jadranska 19, p.p.2964, 1001 Ljubljana, Slovenija
[c] Institut J. Stefan, 1000 Ljubljana, Slovenija

Raziskujeva verjetni mehanizem, zakaj čuti hiperon Λ dvakrat šibkejše jedrsko polje (okrog -27 MeV) kot nukleon (okrog -50 MeV).